

Resolving Ambiguities in the Neutrino Mass-Flavour Spectrum from Supernova Neutrinos

Amol S. Dighe ^a

^aDiv. TH, CERN, CH-1211 Geneva 23, Switzerland.

We analyze the neutrino conversions inside a supernova in the 3ν mixing scheme, and their effects on the neutrino spectra observed at the earth. We find that the observations of the energy spectra of neutrinos from a future galactic supernova may enable us to identify the solar neutrino solution, to determine the sign of Δm_{32}^2 , and to probe the mixing matrix element $|U_{e3}|^2$ to values as low as $10^{-4} - 10^{-3}$.

1. Introduction

In the solutions of the solar and atmospheric neutrino anomalies through the oscillations between the three active neutrino species, three ambiguities remain to be resolved: (i) the solution of the solar neutrino problem – SMA, LMA or VO, (ii) the type of mass hierarchy – normal ($m_3 > m_1, m_2$) or inverted ($m_3 < m_1, m_2$), and (iii) the value of $|U_{e3}|^2$. We show how some of these ambiguities may be resolved from the observations of the neutrino spectra from a Type II supernova.

Only the main results are summarized in this talk. For the detailed arguments and derivations, the reader is referred to [1].

2. Neutrino Conversions

The neutrino transitions between different matter eigenstates inside the supernova take place mainly in the resonance regions H and L , which are characterized by $(\Delta m_{atm}^2, 4|U_{e3}|^2)$ and $(\Delta m_{\odot}^2, \sin^2 2\theta_{\odot})$ respectively. Due to the Δm^2 -hierarchy ($\Delta m_{atm}^2 \gg \Delta m_{\odot}^2$), the dynamics in each of the two resonance layers can be considered independently as a 2ν transition [2]. The final neutrino fluxes can then be written in terms of *survival probabilities* p and \bar{p} of ν_e and $\bar{\nu}_e$ respectively (apart from the geometrical factor of $1/R^2$):

$$\begin{bmatrix} F_e \\ F_{\bar{e}} \\ 4F_x \end{bmatrix} = \begin{bmatrix} p & 0 & 1-p \\ 0 & \bar{p} & 1-\bar{p} \\ 1-p & 1-\bar{p} & 2+p+\bar{p} \end{bmatrix} \begin{bmatrix} F_e^0 \\ F_{\bar{e}}^0 \\ F_x^0 \end{bmatrix}, \quad (1)$$

where $F_e(F_e^0)$, $F_{\bar{e}}(F_{\bar{e}}^0)$ and $F_x(F_x^0)$ are the final (initial) fluxes of ν_e , $\bar{\nu}_e$ and ν_x (each of the non-electron neutrino or antineutrino species) respectively.

Let $P_H(\bar{P}_H)$ and $P_L(\bar{P}_L)$ be the probabilities that the neutrinos (antineutrinos) jump to another matter eigenstate in the resonance layers H and L respectively. The values of p and \bar{p} are determined by these *flip probabilities* and the mixing matrix elements $|U_{ei}|^2$.

The flip probabilities depend on the density profile in the resonance layers. Since $\Delta m^2 < 10^{-2}$ eV² for all transitions, the resonance densities are $\rho_{res} \lesssim 10^4$ g/cc. The resonance layers lie in the outer parts of the mantle, where the density profile may be taken as r^{-3} [3]. Taking $\rho \approx 3.5 \times 10^4$ g/cc $(r/10^9 \text{ cm})^{-3}$ as the density profile, we show in Fig. 1 the contours of equal flip probability P_f in the $(\Delta m^2 - \sin^2 2\theta)$ plot for two different energies on the borders of the observable spectrum. The dependence of the contours on the details of the density profile is very weak [1].

The contours of $P_f = 0.1$ and $P_f = 0.9$ divide the plot into three “regions”. The *adiabatic region* (I), where strong flavour conversions occur, is the region above the contour with $P_f = 0.1$. The *non-adiabatic region* (III), where flavour conversions are almost absent, lies below the $P_f = 0.9$ contour. In the *transition region* (II), the flavour conversions are not complete and the extent of conversions depends on the neutrino energy.

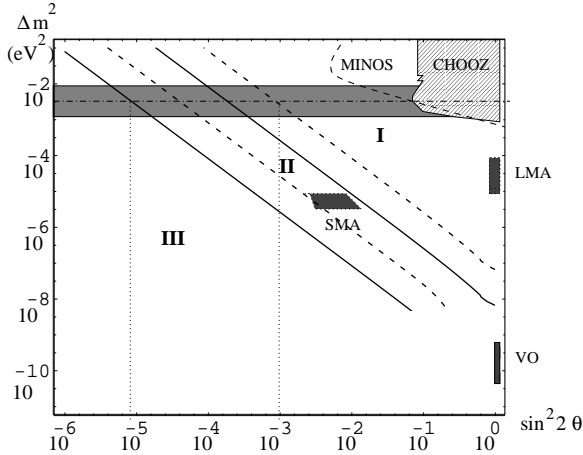


Figure 1. The contours of equal flip probability P_f . The solid (dashed) lines denote the contours of flip probability for a 5 MeV (50 MeV) neutrino: the line on the left stands for $P_f = 0.9$ (highly non-adiabatic transition) and the line on the right stands for $P_f = 0.1$ (adiabatic transition).

The H -resonance lies in the dark horizontal band in Fig. 1, which corresponds to the allowed values of Δm_{31}^2 . The features of the final spectra depend strongly on whether the H -resonance lies in the region I or II (See Table 1). From Fig. 1, the boundary between these regions is at

$$\sin^2 2\theta_{e3} \approx 4|U_{e3}|^2 \sim 10^{-3} \quad , \quad (2)$$

3. Observable effects on the final spectra

The effects of neutrino transitions can be observed through the following features in the neutrino spectra.

(i) The partial or complete disappearance of the ν_e neutronization peak: the ratio of charged to neutral current events during the neutronization burst is directly proportional to p .

(ii) The broadening of the spectra: though the initial (pure) spectra are expected to be “pinched” (have a narrower energy distribution than the Fermi-Dirac one) [4], the final (mixed) spectra need not be pinched. This effective broad-

ening [1] indicates that the final spectrum is composite, *i.e.* the survival probability (p or \bar{p}) is neither very close to 0 nor to 1.

(iii) The earth matter effects: these can be detected through the difference in the energy spectra at two detectors, or through the distortion of the spectrum [1] at a single detector.

The values of the survival probabilities p and \bar{p} are given in Table 1, which illustrate the dependence of the final neutrino spectra on the ambiguities in the neutrino mass-flavour spectrum. From the table, the following observations may be made:

(a) If the neutronization peak in ν_e does not disappear ($p > 0.03 \geq |U_{e3}|^2$), and if the mass hierarchy is known to be the normal one, the H -resonance lies in the region II or III.

(b) If either the final ν_e or $\bar{\nu}_e$ spectrum is determined to be hard (almost the original ν_x spectrum), then the H -resonance is in region I. This gives a *lower* bound on $|U_{e3}|^2$. Moreover, depending on which of the spectrum is the hard one, the type of hierarchy can be determined. A hard ν_e spectrum implies normal hierarchy, a hard $\bar{\nu}_e$ spectrum implies inverted hierarchy.

(c) If both the ν_e and $\bar{\nu}_e$ can be established to be composite (*e.g.* through the observation of broadening), the H -resonance lies in the region II or III.

(d) The observation of any earth matter effects rules out the scenario with the VO solution. If the earth matter effects are observed in the neutrino channels but not in the antineutrino channels, we either have the inverted mass hierarchy, or the normal mass hierarchy with the H resonance in the region II or III.

(e) The observation of earth matter effects in the antineutrino channel identifies the LMA solution. In addition, if the effects are significant in the neutrino channel also, the H resonance can be established to be in the region II or III.

The final neutrino spectra can thus help in resolving the three kinds of ambiguities. In particular, from the observations (a), (c), (d), and (e) above, the H -resonance can be established to be in the region II or III, which implies (eq. 2) an upper bound of $|U_{e3}|^2 < 10^{-4} - 10^{-3}$. This is two orders of magnitude better than the current

Table 1

The values of the survival probabilities p and \bar{p} for various scenarios. $[x, y]$ indicates that the value of the survival probability lies between x and y . In the Earth Matter Effects columns, a \checkmark indicates the possibility of significant earth matter effects.

			Survival Probability		Earth Matter Effects		
			p	\bar{p}	ν_e	$\bar{\nu}_e$	
I	SMA	normal	$ U_{e3} ^2$	1	≈ 0	≈ 0	
		inverted	P_L	$ U_{e3} ^2$	\checkmark	≈ 0	
	LMA	normal	$ U_{e3} ^2$	$\cos^2 \theta_\odot$	≈ 0	\checkmark	
		inverted	$\sin^2 \theta_\odot$	$ U_{e3} ^2$	\checkmark	≈ 0	
	VO	normal	$ U_{e3} ^2$	$[\sin^2 \theta_\odot, \cos^2 \theta_\odot]$	≈ 0	≈ 0	
		inverted	$[\sin^2 \theta_\odot, \cos^2 \theta_\odot]$	$ U_{e3} ^2$	≈ 0	≈ 0	
II	SMA	normal	$[U_{e3} ^2, P_L]$	1	\checkmark	≈ 0	
		inverted	P_L	\bar{P}_H	\checkmark	≈ 0	
	LMA	normal	$\sin^2 \theta_\odot P_H$	$\cos^2 \theta_\odot$	\checkmark	\checkmark	
		inverted	$\sin^2 \theta_\odot$	$\cos^2 \theta_\odot \bar{P}_H$	\checkmark	\checkmark	
	VO	normal	$[U_{e3} ^2, \cos^2 \theta_\odot]$	$[\sin^2 \theta_\odot, \cos^2 \theta_\odot]$	≈ 0	≈ 0	
		inverted	$[\sin^2 \theta_\odot, \cos^2 \theta_\odot]$	$[\sin^2 \theta_\odot \bar{P}_H, \cos^2 \theta_\odot \bar{P}_H]$	≈ 0	≈ 0	
	III	SMA	normal	P_L	1	\checkmark	≈ 0
			inverted	P_L	1	\checkmark	≈ 0
		LMA	normal	$\sin^2 \theta_\odot$	$\cos^2 \theta_\odot$	\checkmark	\checkmark
			inverted	$\sin^2 \theta_\odot$	$\cos^2 \theta_\odot$	\checkmark	\checkmark
		VO	normal	$[\sin^2 \theta_\odot, \cos^2 \theta_\odot]$	$[\sin^2 \theta_\odot, \cos^2 \theta_\odot]$	≈ 0	≈ 0
			inverted	$[\sin^2 \theta_\odot, \cos^2 \theta_\odot]$	$[\sin^2 \theta_\odot, \cos^2 \theta_\odot]$	≈ 0	≈ 0

bound (see CHOOZ in Fig. 1) or that expected from the planned long baseline experiments (see MINOS in Fig. 1).

A galactic supernova may provide us with a sufficient number of events [5] to enable us to reconstruct the energy spectra of ν_e and $\bar{\nu}_e$. Here, we have indicated the observations which can be used in principle to identify various conversion effects. Feasibility studies, involving models for the initial spectra and the detector details, are needed in order to determine what can be achieved in practice.

I would like to thank A. Yu. Smirnov for discussions and insights during the collaboration for [1]. A major part of this work was performed at The Abdus Salam ICTP, Trieste.

REFERENCES

1. A. S. Dighe and A. Yu. Smirnov, hep-ph/9907423.
2. T. K. Kuo and J. Pantaleone, Phys. Rev. **D 37** (1988) 298. S. P. Mikheyev and A. Yu. Smirnov, Prog. Part. Nucl. Phys. **23** (1989) 41.
3. G. E. Brown, H. A. Bethe and G. Baym, Nucl. Phys. **A 375** (1982) 481.
4. E. S. Myra, J. M. Lattimer and A. yahil, Supernova 1987A in the LMC, *ed.* M. Kafatos and A. Michalitsianos, Cambridge University Press, 1988.
5. A. Burrows, D. Klein and R. Gandhi, Phys. Rev. **D 45** (1992) 3361.